Chalcogenide Letters Vol. 20, No. 8, August 2023, p. 587 - 597

Effect of substrate temperature on physical properties of Co doped SnS_2 thin films deposited by ultrasonic spray pyrolysis

Z. Hadef [a,*], K. Kamli[a], O. Kamli [b], S. Labiod [a]
[a]*Department of physics, Faculty of Sciences, University 20 August 1955, BP 26, 21000 Skikda, Algeria*
[b]*Department of mining and geology, Faculty of technology, University of Bejaia, 06000, Bejaia, Algeria*

Ultrasonic Spray Pyrolysis (USP) was used to deposited Co doped SnS_2 thin films on a glass substrate at different substrate temperatures (T_s = 350 °C, 375 °C, 400 °C, and 425 °C). DRX patterns shows that the synthesized films revealed a pure SnS_2 phase with hexagonal structure. The mean crystalline grain sizes were showed an increasing–decreasing trend between 15.67 and 29.84 nm with an increment in the substrate temperature. The SEM images were significantly affected by the substrate temperature. Also, the optical band gap increases from 2.62 to 3.00 eV with the substrate temperatures increasing. Hall Effect measurements confirm the n-type conductivity of the as-deposited films. Furthermore, the films resistivity varies between 117 Ω.cm to 0.20 Ω.cm, as the substrate temperature increases from 350 to 425 °C.

(Received June 7, 2023; Accepted August 14, 2023)

Keyword: SnS_2, Thin films, Physical properties, Spray pyrolysis

1. Introduction

Tin disulfide (SnS_2) is IV-VI binary semiconductor which has developed rapidly within the past few years for its potential applications in photovoltaic devices, due to its photoconductivity properties, less toxic and abundant in nature [1]. Hexagonal structure remains stable for SnS_2 whatever the temperature change, it is a layered material with a cadmium iodide (CdI2) type structure [2]. Thereafter, tin sulfide exists in several phases such as SnS, SnS_2 Sn_2S_3 and Sn_3S_4 lead to bonding characteristics of tin and sulfur, only at higher temperatures (upper to 350° C) the SnS_2 phase appear [32]. It has an n-type conductivity with a wide optical band gap varying between 2.40 and 2.88 eV [3, 4], a light absorber (absorption coefficient up to 10^4 cm^{-1}) and relatively high charge carrier mobility in the range of 18.3 to 230 $cm^2/V.$ s [5]. The optical and electrical properties of SnS_2 films can be improved by doping with impurities [6, 7]. SnS_2 can be explored as a window layer [8] as well as an alternate buffer layer in thin film heterojunction solar cells applications [9]. Several methods are used for the deposition of SnS_2 thin films such as; chemical vapor deposition [10], vacuum evaporation [11], molecular beam epitaxy [12], dip coating technique [13], SILAR [14], and ultrasonic spray pyrolysis [15-19].

The objective of the present work is the study of the substrate temperature effects on the physical properties of the Co doped SnS_2 thin films for photovoltaic applications. It is important to mentioned that the spray pyrolysis technique is the best choice for preparing large-area and low-temperature thin films due to its versatility, viability, and low cost [20].

2. Experimental procedure

2.1. Co doped SnS_2 films preparation

First, the tin disulfide doped silicon thin films were deposited on the soda lime glass substrates (1.0 cm × 1.0 cm) using ultrasonic spray pyrolysis method. Then, 0.1 M of Tin chloride

* Corresponding author: z.hadef@univ-skikda.dz
https://doi.org/10.15251/CL.2023.208.587

($SnCl_4$, $2H_2O$, 1.4827 g) and 0.1 M of Thiourea ($CS(NH_2)_2$, 0.38 g) were dissolved in distilled water (50 mL). The mixture was added to 0.0476 g of Cobalt chloride ($CoCl_2$, $6H_2O$) for prepare Co doped SnS_2thin film. All of the mixtures gave SnS_2 films doped with 4 % Co impurity. The substrates were degreased in successive rinses with ethanol and distilled water. Finally, the obtained solution was sprayed for 40 min on differently heated substrates (T_s) from 350 to 425 °C by an ultrasonic nebulizer which transforms the solution into a stream formed of fine droplets. The ultrasonic vibrator frequency was 40 kHz. The nozzle–substrate distance was kept constant to 4.5 cm during the deposition process.

2.2. Characterization

In present work, the physical properties of SnS_2:Co thin films have been studied by using various techniques. First, the structural analysis of the films was carried out by X-ray diffraction (XRD) with CuKα (λ = 1.5406 Å) radiation. Then, the morphology and chemical composition of the prepared thin films were performed by using a scanning electron microscope (SEM), (FEI Quanta 200), equipped with an energy dispersive spectroscopy (EDS) system. Moreover, optical properties; were studied in the wavelength range 350 – 800 nm using a Cary 5000 UV-Vis-NIR spectrophotometer. Finally, the electrical properties of as deposited films were measured using an HMS-5500 Hall effect measurement system.

3. Results and discussion

3.1. Structural studies

Fig. 1 depicts the XRD pattern of the Co doped SnS_2 thin films deposited at various substrate temperatures (T_s = 350 °C, 375 °C, 400 °C, and 425 °C).

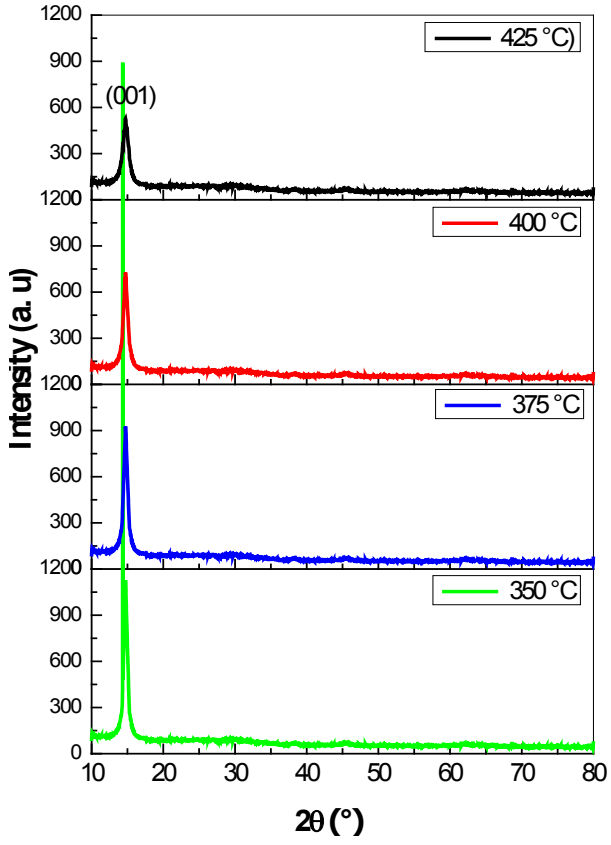

Fig. 1. XRD patterns of Co doped SnS_2 films with various substrate temperatures.

As can be seen that all the films have a polycrystalline structure corresponding to the (001) preferential plane of the SnS_2 hexagonal phase (JCPD data card No. 23-0677) around the angle $2\theta \approx 15.08$. The obtained patterns were not identified peaks that characterized the other phases of tin sulfide and its combination or the metallic Sn and Co because the radius of the Sn^{2+} ion is bigger than that of Co^{2+} ion. Fadavieslam [21] and Yassin et al. [22] have found the same peak (001) for SnS_2 films doped with different impurities (Cu, V, and W) elaborated by spray pyrolysis. Also, similar results were observed about the formation of SnS_2 phase in using other deposition techniques. Kamali [23], Lather et al. [24], Zhang et al. [25], Park et al. [26], and Li et al. [27] found that the phase became predominant as especially for the temperature up to 330◦C. Comparison of the four curves indicates that the intensity of the preferred peak decreases with the substrate temperature increasing. The decrease in peak intensity is probably due to its broadening; which amounts to an overlap of very small peaks; in other words, the emergence of new peaks to the detriment of the preferential orientation.

The lattice parameters *a* and *c* of hexagonal structure were determinated from XRD patterns data according to the following relationship [28]:

$$\frac{1}{d_{hkl}^2} = \frac{4}{3}\left(\frac{h^2+hk+k^2}{a^2}\right) + \frac{l^2}{c^2} \quad (1)$$

The lattice parameters of all diffraction XRD peaks corresponding to the various substrate temperatures of Co doped SnS_2 films were estimated. It is observed that the evaluated values of *a* and *c* are in good agreement with those given in the standard card of SnS_2 (JCPDS N◦: 23-0677). The calculated *c/a* ratio was always found slightly higher than the standard value (1.6170) of the hexagonal structure. This may be caused by the doping effect of Co impurities in the SnS_2 crystal, which causes local changes in the lattice parameters. Table 1 summarized the obtained results.

The crystallite size (D) of the SnS_2:Co thin films was determinated from XRD patterns by using the Debye-Scherrer formula [29]:

$$D = \frac{k\lambda}{\beta \cos\theta} \quad (2)$$

where $k = 0.94$ is the shape factor, λ is the wavelength of CuKα radiation source ($\lambda = 1.5406$ Å), β is the (full width half maxi-mum) FWHM value of the respective diffraction peak, and θ is the Bragg angle. The crystallite size values of Co doped SnS_2 thin films are lower than that of pure SnS_2 even with the change of substrate temperature [32]. Because Sn^{2+} has a bigger ionic radius then Co^{2+}. So, the Cobalt ion occupies interstitial positions, compacting the unit cell [30].

Table 1. Structural parameters of spray ultrasonic Co doped SnS_2 film.

T_s (°C)	*h k l* planes	Lattice Param. (Å)		*c/a*	Standard (JCPD No. 23-0677)
		a	*c*		
350	001	3.613	5.887	1,6294	a = 3.648 A° c = 5.899 A° c/a = 1.6170
375		3.623	5.905	1,6299	
400		3.603	5.872	1,6298	
425		3.628	5.914	1,6301	

The strain (*ε)* developed in the deposited samples was estimated by using the following relation [31]:

$$\varepsilon = \frac{\beta \cos\theta}{4} \quad (3)$$

The dislocation density (δ), defined as the length of dislocation lines per unit volume of the crystal is calculated using the Williamson and Smallman's formula [32].

$$\delta = \frac{1}{D^2} \quad (4)$$

The obtained results of structural parameters are summarized in Table 2.

Table 2. Regroups calculated values of crystallite size (D), dislocation density (δ) and the strain (ε) using XRD spectra of Co doped SnS_2 films.

T_s (°C)	d (Å)	D (nm)	ε (x10^{-3})	δ ×10^{-4} (lines.nm^{-2})
350	5.912	15,67	2,21	40.72
375	5.903	19,10	1,81	27.41
400	5.881	25,41	1,36	15.50
425	5.869	18,84	1,84	28.17

Fig. 2 illustrates the variations of the crystallite size and the lattice strain. The obtained results showed that the evolution of the crystallites size has an inversely proportional relationship to the lattice strain.

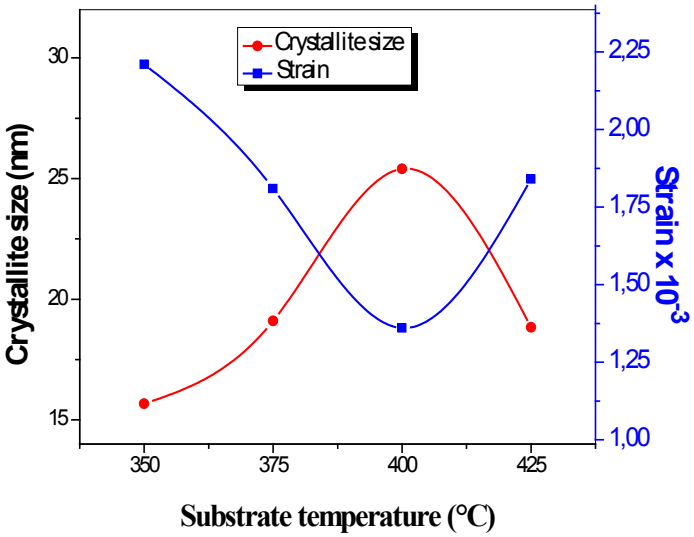

Fig. 2. Variation of crystallite size and Strain of Co doped SnS_2 films elaborated at different substrate temperature (T_s = 350 °C, 375°C, 400 °C and 425 °C).

The crystallite size of the Co doped SnS_2 films increases from 15.67 nm to 25.4 nm with the substrate temperature increasing from 350 to 400 °C then decreases to 18.84 for 425 °C. Lather et al. [24] have found the same order of crystallite size for Zn doped SnS_2 films with variation of Zn concentration and Hadef et al. [3] have found the similar results for SnS_2 films with variation of substrate temperature. The distance between the crystal planes decreases with the substrate temperature increasing. However, the crystallite size trend is reversed at higher temperature T_s = 425 °C. This may be attributed to the structural defects increasing (strain, and dislocation density) in the films.

3.2. Morphological studies

The SEM micrographs of SnS_2 thin films doped with Co impurities at various substrate temperatures are illustrated in Fig. 3.

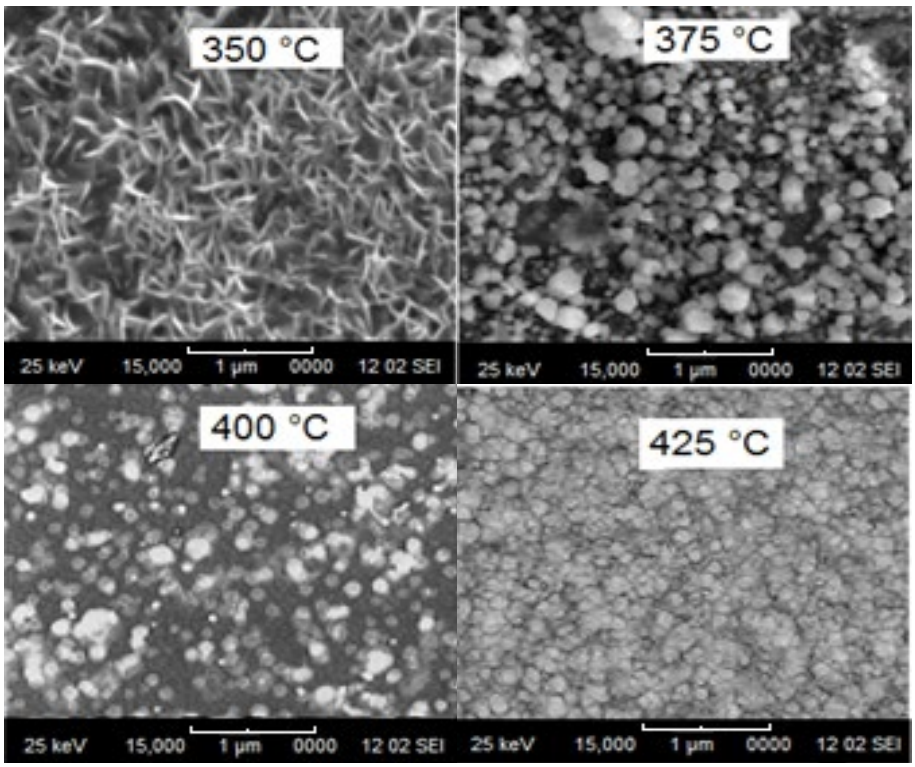

Fig. 3. SEM images of Co doped SnS_2 thin films deposited at different substrate temperatures.

The SEM micrographs showed that the as-deposited film at T_s= 350 °C exhibited platelet-shaped grains smaller in size randomly oriented. Similar Platelet- shaped grains for SnS_2 films were also observed by Voznyi et al. [5] Chalapathi et al. [9]. It is clear that the films have a granular morphology and uniform surface devoid of cracks with substrate temperature increasing up to 375 °C. In fact, the growth of clusters was observed in all other samples caused by the effect of Cobalt in enhancing the surface topography of the films, because the addition of Cobalt atoms to the deposited solution with increasing the temperature led to their coalescence and hence the formation of larger grain sizes. This granular morphology was observed by Fadavieslam [21] for sprayed Cu doped SnS_2 films with variation of substrate temperature. The SEM images exhibited that the surface morphology of the Co doped SnS_2 films strongly dependent on the substrate temperature. The obtained average grain sizes from the SEM images are 161, 174, and 166 nm at different substrate temperatures of 375, 400 and 425 °C respectively. It is clear that the dense structure is formed which caused by the well bonding between the grains.

Table 3. EDS measurements of Co doped SnS_2 thin films for different substrate temperatures.

T_s (°C)	350	375	400	425
S (at. %)	58.88	53.80	48.82	44.78
Sn (at. %)	40.30	45.18	50.08	54.03
Co (at. %)	0.82	1.02	1.10	1.19
Sn/S	0.68	0.85	1.02	1.21

The chemical properties of Co doped SnS_2 thin films deposited at various substrate temperature are analyzed by using Energy Dispersive Spectroscopy (EDS). Several points on the surface and the atomic percentage of Sn, S, and Co are selected. The obtained results are gathered in Table 3.

The presence of Sn, S and Co elements confirms the near stoichiometric composition of the as-deposited films. Other elements such as O, N, C and Cl exist, but with a very low amount causing no alternance in the film properties. The existence of Cl, C and N is a clear signature that the $SnCl_4$, $CoCl_2$ and CS $(NH_2)_2$ are not completely consumed at the used substrate temperature of 425 °C. The oxygen may originate from water and thiourea. Ttypical EDS spectra of Co doped SnS_2 film deposited at T_s = 425 °C is shown in Fig. 4.

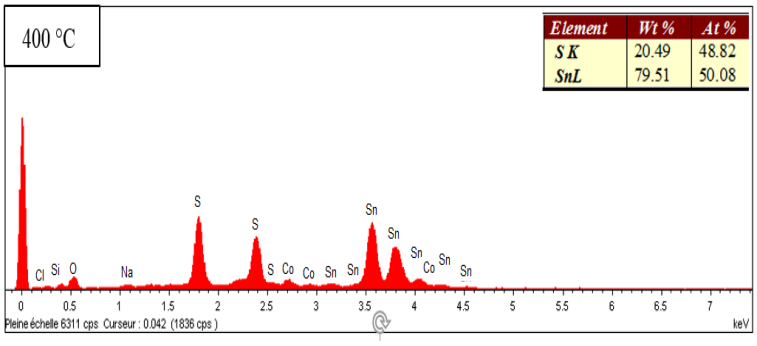

Fig. 4. EDS spectra of Co doped SnS_2 thin films deposited at T_s = 425 °C.

The Sn/S ratio is estimated from the EDS analysis of Co doped SnS_2 films deposited at various substrate temperatures. The obtained results indicate that elaborated films become sulfur deficient with the increase of the substrate temperatures. Therefore, the elaborated films at lower temperatures are sulfur rich in nature with Sn/S ratio of 0.68 for T_s = 350 °C. Moreover, with the increasing of temperature, a near stoichiometry is obtained between Sn and S elements (Sn/S ratio becomes higher than 1 for T_s up to 400 °C). This variation in chemical composition from quasi-stoichiometric to stoichiometric in the Co doped SnS_2 films with the substrate temperatures increasing is attributed mainly to the re-evaporation of sulfur atoms due to the high temperature [33, 34].

3.3. Optical studies

The optical properties of the Co doped SnS_2 thin films such as; transmittance (T), absorbance (α), band gap energy (E_g) and refractive index (n) are investigated. Fig. 5 illustrates the optical transmittances as function of incident light wavelength.

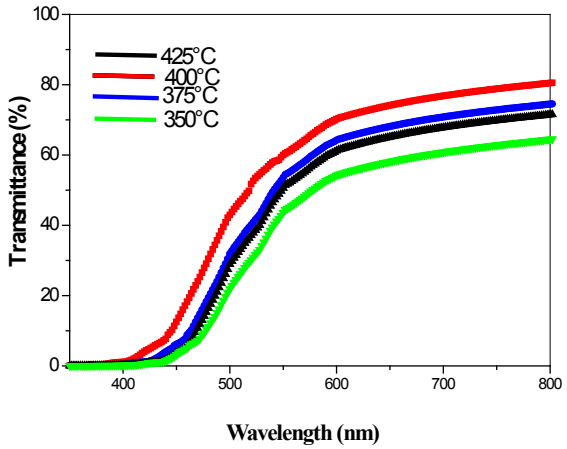

Fig. 5. Transmittance spectra of Co doped SnS_2 films prepared at different substrate temperatures.

It can be seen that the transmittance is increased with the substrate temperature increasing. All the grown films exhibited a mean optical transmittance approximately 60-80 %. This result allows the use of Co doped SnS_2 thin films in photovoltaic applications. The absence of interferences fringes in the transmittance spectra indicates that the films have rough surfaces.

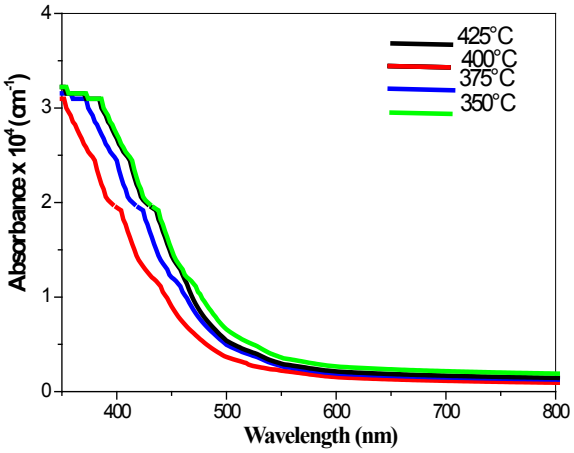

Fig. 6. Absorbance spectra of Co doped SnS_2 films deposited at various substrate temperatures.

Absorption coefficient decreases exponentially with an increase in wavelength region of 350–800 nm as shown in Fig. 6. The better crystallinity of the films is again established from the sharp decrease in absorption spectra in near the band edge.

Optical band gaps of Co doped SnS_2 films are estimated from Tauc relationship [35]:

$$(\alpha h\nu^2 = A(h\nu - E_g) \tag{5}$$

where h is Planck's constant, ν is photon frequency, α is absorption coefficient, E_g is energy gap, and A represents the proportionality constant. The graph of $(\alpha h\nu)^2$ versus photon energy for Co doped SnS_2 thin films prepared at various substrate temperatures is shown in Fig. 7.

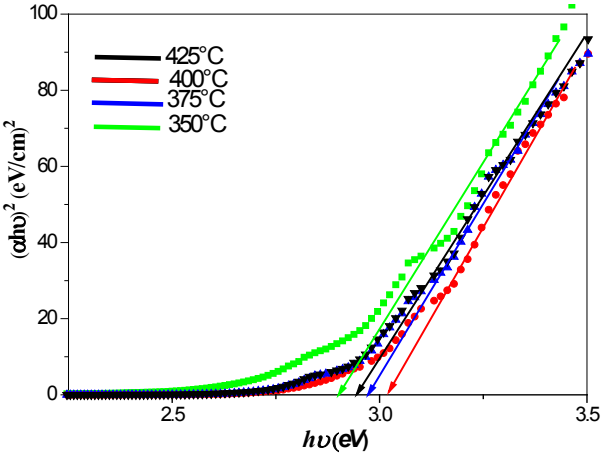

Fig. 7. Variation of $(\alpha h\nu)^2$ as a function of the photon energy ($h\nu$).

The linear correlation between $(\alpha h\upsilon)^2$ and hυ at higher energies demonstrates that the obtained Co doped SnS_2 films are essentially direct transition type semiconductors. The estimated band gap values are shown in Fig. 8.

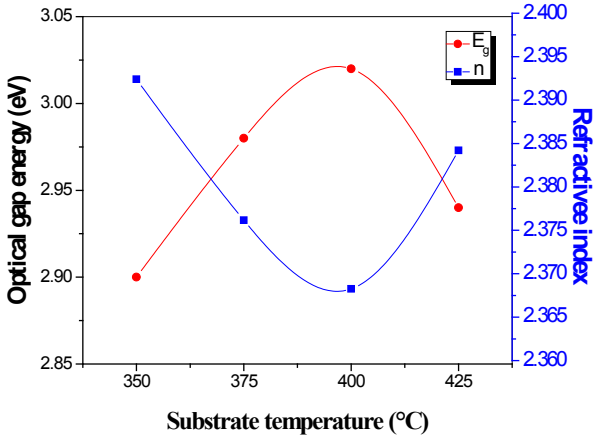

Fig. 8. Variation of optical energy band gap and refractive index as function of substrate temperature.

It is increased from 2.90 to 3.02 eV as the substrate temperature increases from 350 °C to 400 °C then decreased to 2.94 eV for 425 °C. The increase in band gap value can be caused by the variation in localized state density in the energy gap indicates an improvement in crystallinity and vice versa [36, 37].

Refractive index (n) of Co doped SnS_2 thin films was calculated by using Moss model [38], represented by a general relationship which is based on the concept that in a dielectric, energy levels are scaled by a factor ε_∞^2, (where $\varepsilon_\infty = n^2$ is the optical dielectric constant):

$$n^4 E_g = 95\ eV \tag{6}$$

Fig. 8 shows again the variation in refractive index of Co doped SnS_2 films deposited with varying substrate temperature. It is varied between 2.37 to 2.39 as the substrate temperature increases from 350 to 425 °C. The addition of Co impurities accompanied by an increase in temperature caused a dense packing of particles that hinders the propagation of light through [37].

3.4. Electrical properties

Hall Effect measurement was used to determine the electrical properties of Co doped SnS_2 films, it is an important test in the photovoltaic field to determine its maximum benefit in solar energy conversion. The influence of the substrate temperature has been investigated based on the resistivity, conductivity, Hall mobility, carrier density, and the conductivity type of the films, the obtained results were listed in Table 4.

Table 4. Summarizes values of electrical proprieties of Co doped SnS_2 films.

T_s (°C)	Resistivity (Ω.cm)	Conductivity ($\Omega^{-1}.cm^{-1}$)	Mobility (cm^2/Vs)	Carrier density x 10^{17} (cm^{-3})	Type cond.
350	117	8.54 x10^{-3}	04.83	3.62	n
375	18.9	5.29 x10^{-2}	08.48	4.73	n
400	0.20	5.00	38.68	6.57	n
425	21.1	4.73 x10^{-2}	07.15	4.43	n

The electrical resistivity of Co doped SnS_2 films reveals a significant decrease in value from 117 to 0.20 Ω.cm with substrate temperature increasing from 350 to 400 °C then increases to 21.1 Ω.cm for T_s = 425 °C. The n- type conductivity is confirmed from the Hall measurements of the films. In addition, Hall mobility shows an increasing-decreasing trend with estimated values of 4.83, 8.48, 38.68 and 7.15 cm^2/Vs at 350, 375, 400 and 425°C, respectively. Also, the carrier density depicts the similar behaviour at the same substrate temperatures with determinated values of 3.62 x10^{17}, 4.73 x10^{17}, 6.57 x$10^{17}$and 4.43 x10^{17} cm^{-3}. This change in electrical properties of the as-deposited films is in accordance with the changes observed in the grain size and crystallinity as substrate temperature is varied. Therefore, high conductivity of the Co doped SnS_2 film is about 5.00 Ω^{-1} cm^{-1} obtained at 400 °C which is attributed to improved crystallization in accordance with XRD results. Same trend in the variation of electrical proprieties is reported on Cu doping [21] in SnS_2 deposited using spray pyrolysis technique at various substrate temperatures.

4. Conclusion

In present study, ultrasonic spray pyrolysis was used to deposit Co doped SnS_2 thin films with varying substrate temperature at 350, 375, 400 and 425 °C. The XRD patterns indicate that the films have a hexagonal structure having preferential orientations along (001) planes. Also, the crystallite size has an increasing-decreasing trend in range of 15,67 - 25,41 nm with substrate temperature increasing. The SEM images indicate that the Co doped SnS_2 films have a granular morphology which gives a dense structure leading to the formation of larger grains. Optical studies were revealed the direct dependence of optical band gap with the substrate temperature, the calculated band gap values were increased from 2.90 to 3.02 eV as the substrate temperature increases from 350 °C to 400 °C then were decreased to 2.94 eV for 425 °C. The Hall Effect measurements was showed that the films are n-type in nature. The resistance of the thin films was revealed a significant decrease from 117 to 0.20 Ω.cm with the substrate temperature increasing from 350 to 400 then was decreased to 21.1 Ω.cm at 425°C. Moreover, the carrier density mobility and of the films exhibits an increase–decrease trend with the substrate temperature increasing. Considering the obtained results, it can be concluded that the physical properties Co doped SnS_2 can be well affected by the variation of the substrate temperature.

References

[1] N. Anitha, M. Anitha, L. Amalraj, Optik **148**, 28 (2017); https://doi.org/10.1016/j.ijleo.2017.08.139
[2] M.N. Amroun, M. Khadraoui, Optik **184**, 16 (2019); https://doi.org/10.1016/j.ijleo.2019.03.011
[3] Z. Hadef, K. Kamli, B. Zaidi, S. Boulkhessaim, B. Chouial, Journal of Nano Research **77**, 105 (2023); https://doi.org/10.4028/p-2rx1mg
[4] I. Bouhaf Kherchachi, H. Saidi, A. Attaf, N. Attaf, A. Bouhdjar, H. Bendjdidi, Y. Benkhetta, R. Azizi, M. Jlassi, Optik **127**, 4043 (2016) ; https://doi.org/10.1016/j.ijleo.2016.01.120
[5] Voznyi A, Kosyak V, Opanasyuk A, N. Tirkusova, L. Grase, A. Medvids, G. Mezinskis, Materials Chemistry and Physics **173**, 52 (2016); https://doi.org/10.1016/j.matchemphys.2016.01.036
[6] A.M.S. Arulanantham, S. Valanarasu, S. Rex Rosario, A. Kathalingam, M. Shkir, V. Ganesh, I.S. Yahia , Journal of Materials Science: Materials in Electronics **30**, 13964 (2019); https://doi.org/10.1007/s10854-019-01743-w
[7] B.K. Rajwar, S.K. Sharma, Optical and Quantum Electronics **54(2)**, 1 (2022); https://doi.org/10.1007/s11082-021-03424-7
[8] K. Kamli, Z. Hadef, B. Chouial, B. Hadjoudja, Global Journals of Research in Engineering **17(J5),** 37 (2017); https://engineeringresearch.org/index.php/GJRE/article/view/1721
[9] U. Chalapathi, B. Poornaprakash, B. Purushotham Reddy, Thin Solid Films **640**, 81 (2017); https://doi.org/10.1016/j.tsf.2017.09.004
[10] R.D. Engelken, H.E. McCloud, C. Lee, M. Slayton, H. Ghoreishi, Journal of The Electrochemical Society **134,** 2696 (1987); https://doi.org/10.1149/1.2100274
[11] K. Kawano, R. Nakata, M. Sumita, Journal of Physics D: Applied Physics **22**, 136 (1989); https://doi.org/10.1088/0022-3727/22/1/019
[12] R. Schlaf, N.R. Armstrong, B.A. Parkinson, C. Pettenkofer, W. Jaegermann, Surface Science **385**, 1 (1997); https://doi.org/10.1016/S0039-6028(97)00066-6
[13] S.K. Panda, A. Antonakos, E. Liarokapis, S. Materials Research Bulletin **42**, 576 (2007); https://doi.org/10.1016/j.materresbull.2006.06.028
[14] N.G. Deshpande, A.A. Sagale, Y.G. Gudage, C.D. Lokhande, R. Sharma, Journal of Alloys and Compounds **436**, 421 (2007); https://doi.org/10.1016/j.jallcom.2006.12.108
[15] K. Kamli, Z. Hadef, B. Chouial, B. Zaidi, B. Hadjoudja, A. Chibani, Surface Engineering **33**, 567 (2017); https://doi.org/10.1080/02670844.2016.1271593
[16] Z. Hadef, K. Kamli, A. Attaf, M.S. Aida, B. Chouial, Journal of Semiconductors **38**, 063001 (2017); https://doi.org/10.1088/1674-4926/38/6/063001
[17] K. Kamli, Z. Hadef, B. Chouial, B. Hadjoudja, Surface Engineering **35**, 86 (2019); https://doi.org/10.1080/02670844.2018.1475052
[18] N. Houaidji, M. Ajili, B. Chouial, N. Turki Kamoun, K. Kamli, A. Khadraoui, B. Zaidi, B. Hadjoudja, A. Chibani, Z. Hadef, Journal of Nano Research **60**, 63 (2019); https://doi.org/10.4028/www.scientific.net/JNanoR.60.63
[19] B. Zaidi, N. Houaidji, A. Khadraoui, S. Gagui, C. Shekhar, Y. Ozen, K. Kamli, Z. Hadef, M. Donmez, B. Comert, B. Chouial, B. Hadjoudja, Journal of Nano Research **61**, 72 (2020); https://doi.org/10.4028/www.scientific.net/JNanoR.61.72
[20] L. Amalraj, C. Sanjeeviraja, M. Jayachandran, Journal of Crystal Growth **234**, 683 (2002); https://doi.org/10.1016/S0022-0248(01)01756-0
[21] M.R. Fadavieslam, Journal of Semiconductors **39**, 123005 (2018); http://dx.doi.org/10.1088/1674-4926/39/12/123005
[22] O.A. Yassin, A.A. Abdelaziz, A.Y. Jaber, Materials Science in Semiconductor Processing **38**, 81 (2015); http://dx.doi.org/10.1016/j.mssp.2015.03.050
[23] K Kamali, Materials Research Bulletin **150**, 111757 (2022); https://doi.org/10.1016/j.materresbull.2022.111757
[24] R. Lather, P. Jeevanandam, Journal of Alloys and Compounds **891**, 161989. (2021); https://doi.org/10.1016/j.jallcom.2021.161989

[25] F. Zhang, Y. Zhang, Y. Wang, A. Zhu, Y. Zhang, Separation and Purification Technology **283**, 120161 (2022); https://doi.org/10.1016/j.seppur.2021.120161
[26] J.H. Park, J.C. Ro, S.J. Suh, Current Applied Physics **42**, 50 (2022); https://doi.org/10.1016/j.cap.2022.08.005
[27] Z. Li, W. Shu, Q. Li, W. Xu, Z. Zhang, J. Li, Y. Wang, Y. Liu, J. Yang, K. Chen, X. Duan, Z. Wei, B. Li, Advanced Electronic Materials, 7, 2001168 (2021); https://doi.org/10.1002/aelm.202001168
[28] B.R. Sankapal, R.S. Mane, C.D. Lokhande, Materials Research Bulletin, 35, 2027 (2000); https://doi.org/10.1016/S0025-5408(00)00405-0
[29] L.I. Maissel, R. Glang, P.P. Budenstein1, Journal of The Electrochemical Society 1**18**, 114C (1971); https://doi.org/10.1149/1.2408101
[30] A. Jrad. T. Ben Nasr, N. Turki Kamoun, Optical Materials **50**, 128 (2015); https://doi.org/10.1016/j.optmat.2015.10.011
[31] M.R.A. Bhuiyan, M.A.A. Azad, S.M.F. Hasan, Annealing effect on structural and electrical properties of AgGaSe2 thin films, Indian Journal of pure and Applied Physics **49** (2011) 180-185.
[32] N. Houaidji, M. Ajili, B. Chouial, N. Turki Kamoun, K. Kamli, A. Khadraoui, Z. Hadef, B. Zaidi, B. Hadjoudja, Journal of Nano Research **65**, 13 (2020); https://doi.org/10.4028/www.scientific.net/JNanoR.65.13
[33] Z. Hadef, K. Kamli, Materials Today Proceedings **49**, 1079 (2022); https://doi.org/10.1016/j.matpr.2021.09.330
[34] M. Devika, N. Koteeswara Reddy, D. Sreekantha Reddy, Q. Ahsanulhaq, K. Ramesh, E.S.R. Gopal, K.R. Gunasekhar, Y.B. Hahn, Journal of The Electrochemical Society **155**, H130 (2008); https://doi.org/10.1149/1.2819677
[35] J. Tauc, R. Grigorovici, A. Vancu, Physica Status Solidi b **15**, 627 (1966); http://dx.doi.org/10.1002/pssb.19660150224
[36] K.t. Ramakrishna Reddy, G. Sreedevi, R.W. Miles, Journal of Materials Sciences and Engineering A **3**, 182 (2013); http://dx.doi.org/10.1155/2013/528724
[37] S. Gedi, V.R. Minnam Reddy, C. Park, J. Wook, K.T. Ramakrishna Reddy, Optical Materials **42**, 468 (2015); http://dx.doi.org/10.1016/j.optmat.2015.01.043
[38] T.S. Moss , Physica status solidi b **131**, 415 (1985); https://doi.org/10.1002/pssb.2221310202